

Traffic Flow Management Impact on Delay and Fuel Consumption: an Atlanta Case Study

Shon R. Grabbe, Banavar Sridhar, Avijit Mukherjee,
and Alexander Morando

In 2010, the FAA investigated the use of a capability called a Traffic Management Advisor Flow Programs to control flights destined for capacity-limited airports. This study explores through fast-time simulations the impact of this new capability on Hartsfield-Jackson Atlanta International Airport arrival operations. The emphasis of this study is on examining the distribution of delays and emissions for flights included and exempted from this new capability. To determine the “best” flow rate to select when developing a Traffic Management Advisor Flow Program, a simulation-based approach is presented. This approach depends on the arrival demand, airport configuration, acceptance rate, and program goals. When the goal was to balance delays between flights included and exempt from the program, then a flow rate of 60 aircraft per hour was recommended. When the goal was to minimize overall system delays, however, then a flow rate that was 33% higher was recommended. Complementing the flow rate recommendation analysis was an activity designed to assess the environmental impacts of first scheduling Atlanta arrivals with a Traffic Management Advisor Flow Program and subsequently by the Traffic Management Advisor. A strong correlation between the Traffic Management Advisor Flow Program flow rate and the fuel burn and emissions associated with the Traffic Management Advisor delays was observed. When the Traffic

Shon R. Grabbe and Banavar Sridhar are with NASA Ames Research Center, Moffett Field, CA. Avijit Mukherjee and Alexander Morando are with the University of California, Santa Cruz.

Received July 15, 2011; accepted July 27, 2012.

Air Traffic Control Quarterly, Vol. 20(3) pp. 203–224 (2012)

CCC 1064-3818/95/030163-20

Management Advisor Flow Program flow rate was increased from 54 aircraft per hour to 80 aircraft per hour, the fuel burn and emissions associated with airborne holding was found to increase by over 100%. This increase in fuel burn or emissions, in general, represents a small percent of the total fuel burn and emissions associated with the entire flight's trajectory, and only a percent of all arrivals were assigned airborne holding. Aviation's impact on the environment is a pressing matter, and the design of Traffic Flow Management control strategies will require considering the delays as well as the emissions resulting from them.

INTRODUCTION

When the demand at an airport significantly exceeds the available capacity, the Traffic Management Advisor (TMA) [Swenson, et al., 1997] assigns delays to arriving flights to moderate the demand to current or anticipated capacity levels. For reference, the TMA is a decision support tool deployed throughout the United States for efficiently sequencing and scheduling aircraft to arrival meter fixes, final approach fixes, and to the runway threshold, while taking into account the airport configuration, the winds aloft, aircraft types, and separation and/or flow rates constraints. These delays can lead to inefficiencies and significantly increase the complexity associated with managing the traffic flows in the en route environment. When this occurs, additional traffic management initiatives such as Ground Delay Programs (GDPs) have historically been implemented. One major downside associated with controlling flights with both a GDP and the TMA is that flights departing from within the same Center in which they later land can be “double delayed” (i.e., flights can receive multiple uncoordinated pre-departure delays from the two systems) [Duquette and Lacher, 2010; Grabbe et al., 2010].

To mitigate this “double penalization” problem, the FAA investigated the use of a capability called a Traffic Management Advisor Flow Program (TFP) in 2010. This new capability reduces the demand of flights destined for a capacity limited airport by assigning pre-departure delays. Here the flights controlled by the TFP depart from outside of the TMA scheduling horizon, which typically extends about 200 nmi from the airport. This new capability allows traffic flow managers to exempt internal departures from the TFP, which alleviates the double penalization problem.

Figure 1 illustrates the key differences between a TFP and a more conventional GDP for three sample flights that are destined for Hartsfield-Jackson Atlanta International Airport (ATL) while TMA is operating at ATL. Under a GDP scenario (see Figure 1a), the set of controllable flights can be specified by an exemption radius, which is illustrated by the gray circle in Figure 1a. All flights outside this circle are generally exempt from the GDP (see for example, “ac₃” in Figure 1a), while flights within the circle (see for example, “ac₁” in

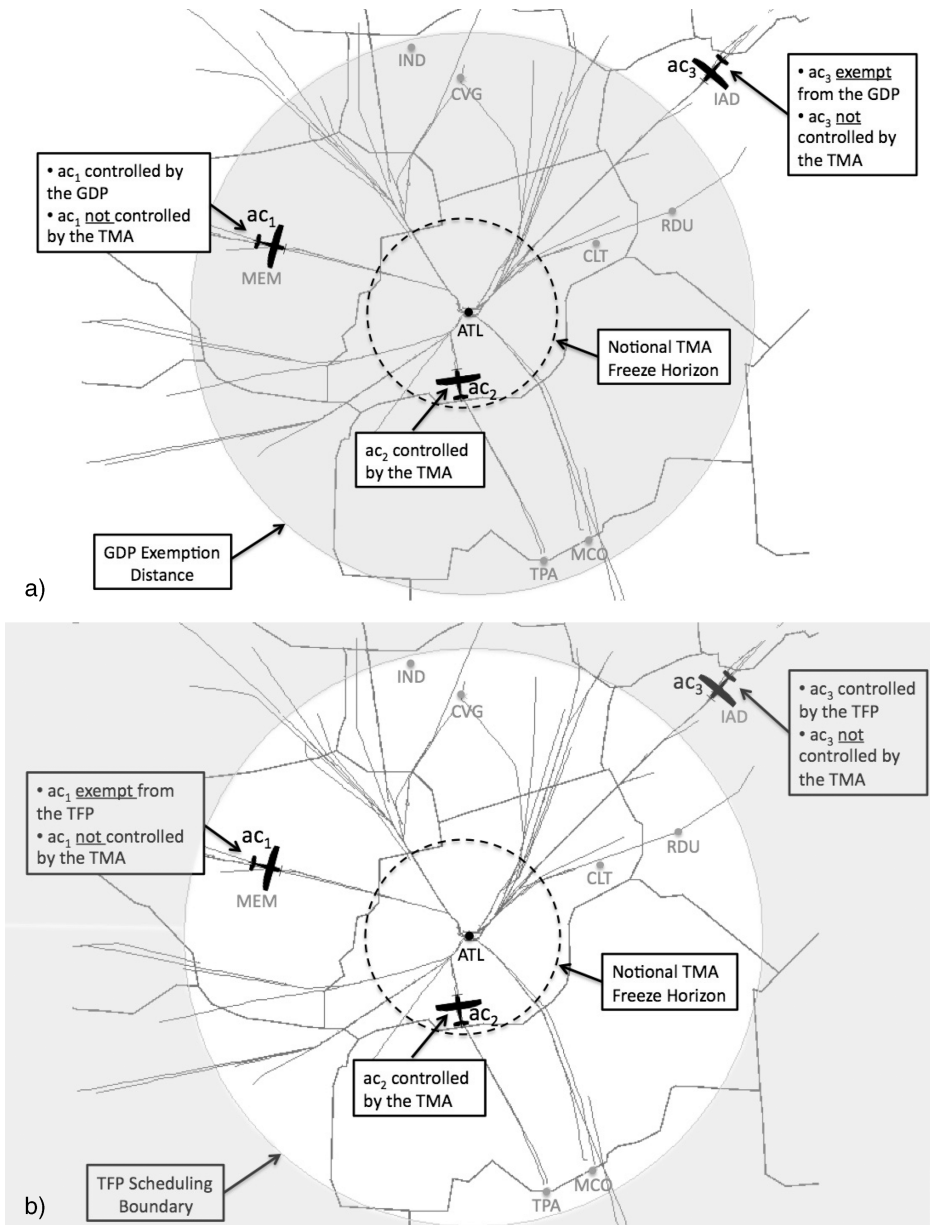


Figure 1. Notional scenario to illustrate the key differences between a Ground Delay Program (Figure 1a) and a Traffic Management Advisor Flow Program (Figure 1b) operated in conjunction with the Traffic Management Advisor.

Figure 1a) are candidates for being assigned a pre-departure delay by the GDP. In contrast, when a TFP is operated at an airport, the flights within the white circle (see for example, “ac₁” in Figure 1b) are typically exempt from the TFP, while flights outside the circle are candidates for being assigned a pre-departure delay (see for example, “ac₃” in Figure 1b). Regardless of whether a GDP or a TFP is being

operated at an airport, all arrivals are subsequently scheduled by the TMA once the flights reach the TMA freeze horizon (see for example, “ac₂” in Figure 1), which is depicted by the dashed circle in Figure 1.

Since the TFP is relatively new (i.e., the first one was investigated at Newark Liberty International Airport (EWR) in April 2010), few published studies have examined the effectiveness of this new capability. In [Duquette and Lacher, 2010], the effectiveness of the first trial of the TFP concept for EWR arrivals was analyzed. Subsequently in [Grabbe et al., 2011], an integrated fast-time modeling and simulation system was introduced to explore the distribution of delays incurred by flights included and exempt from a TFP that was designed to control ATL arrivals. Additional research studies that are designed to investigate TFPs would greatly improve the operational utility and effectiveness of this new capability.

To address this research gap, an integrated fast-time simulation system that consists of NASA’s Future ATM Concepts Evaluation Tool (FACET) [Bilimoria, et al., 2001], the FAA’s Flight Schedule Monitor (FSM) [ETMS, 2005], the TMA, and an environmental impact model [Sridhar et al., 2011] has been developed. Within this integrated system, FACET was used to model the flow of traffic in the National Airspace System (NAS); the FSM was used to plan the TFP; the TMA sequenced and scheduled the arrivals within about 200 nmi of the destination airport and the environmental impact model calculated the aircraft fuel burn and emissions. Using this system, operationally derived scenarios were developed to investigate the impact that TFPs can have on one of the world’s busiest airports, ATL. For reference, the FAA proposed the use of a TFP to manage arrival demand at ATL during periods of taxiway construction in the fall of 2010. Results are presented in terms of the distribution of delays, fuel burn, and emissions imposed by the Traffic Flow Management (TFM) controls associated with the TFP and the TMA.

The Modeling Methodology section describes the software architecture of the integrated decision support capability and the environmental impact model. A discussion of the TFP scenarios, the simulation inputs, and the TMA settings is presented in Experimental Setup section. The experimental results of fast-time simulations used to explore the uncoordinated impacts of the TFP and the TMA on arrivals into ATL are presented in the Results section. Finally, the paper ends with the Conclusions section.

MODELING METHODOLOGY

The simulation system used to explore the TFPs at ATL and the environmental impact model used to calculate aircraft fuel burn and emissions are described in this section.

Simulation System

The major components of the integrated software system that was developed to explore interactions between the TMA and the TFP are illustrated in Figure 2. On the left side of this figure are the system inputs, which consist of user schedules and flight plans and airspace adaptation data. The user schedules were extracted from historical Aircraft Situation Display to Industry (ASDI) data archives that will be described in the Experimental Setup section. The adaptation data for the “Primary Simulation” system was extracted from the FAA’s Traffic Flow Management System (TFMS) [ETMS, 2005].

These system inputs were processed directly by the “Primary Simulation” system, FACET. Every 20 seconds of simulation time, the “Primary Simulation” provides updated state information, $x(t)$, (e.g., latitude, longitude, speed, altitude, and heading) for all aircraft in the simulation via an Application Programming Interface (API) that has been described in previous studies [Grabbe et al., 2009]. This state information is used directly by the “Fuel Burn and Emissions Model” to calculate the fuel burn and the following emissions: carbon monoxide (CO), carbon dioxide (CO₂), hydrocarbons (HC), oxides of nitrogen (NO_x), water vapor (H₂O) and oxides of sulfur (SO_x). More details regarding the fuel burn and emissions model are provided in the next subsection.

For this initial study, the interactions between FACET and the FSM were accomplished via file transfer. Prior to conducting the fast-time simulation experiments, the TFP was planned in FSM and the resulting flight controls, which consisted of a set of Controlled Times of Departure (CTDs) for all flights included in the TFP, were logged to a file. For reference, this set of flights will be described in detail in the Experimental Setup section. This file was

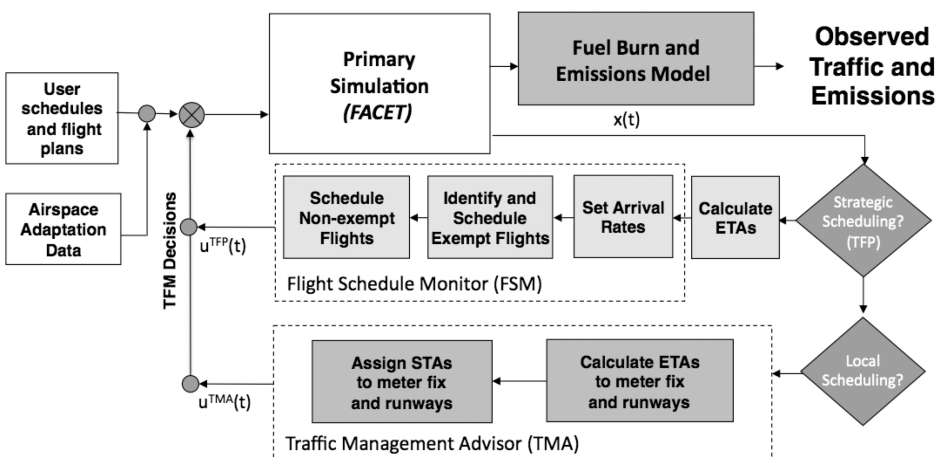


Figure 2. Integrated system architecture.

subsequently read by a Java-based application that communicated with FACET via the FACET API in order to implement the TFP controls, $u^{TFP}(t)$.

The first step in planning the TFP consists of calculating Estimated Times of Arrival (ETAs) for all flights to the boundary of the Flow Constrained Area (FCA) associated with the TFP. The definition of the FCA for the ATL scenario will be described in the Experimental Setup section. Operationally, and for this study, the ETAs are calculated by the TFMS and transferred via an Aggregate Demand List (ADL) file to FSM. The four boxes that are collectively labeled as the “Flight Schedule Monitor” in Figure 2 illustrate the high-level steps associated with planning a TFP in FSM. Once the ETAs have been transferred to FSM, a human operator subsequently sets the FCA arrival rate via the FSM interface. In the box labeled “Identify and Schedule Exempt Flights,” all flights exempt from the TFP are specified via the FSM interface, and the Controlled Times of Arrival (CTAs) associated with these flights are set to the ETAs. The list of flights exempt from the ATL scenario is described in the Experimental setup section. Lastly, the Ration-by-Schedule (RBS) algorithm resident in FSM is used to calculate CTAs and CTDs for all non-exempt flights in the box labeled “Schedule Non-Exempt Flights” in order to satisfy the flow rate constraints at the FCA boundary. These controls are subsequently logged to an auxiliary file that is read by FACET.

The actual merging and spacing of the traffic flows to ensure efficient usage of the airport runways is accomplished via the collection of boxes labeled “Traffic Management Advisor” in Figure 2. For the current study, the TMA performs the activities associated with these boxes once every 20 seconds. It is worth noting that operationally, TMA receives real-time position updates every twelve seconds, which coincides with the Center radar update rate. The slower update rate was selected for the fast-time simulations to improve computational performance. Using the trajectory prediction capabilities of TMA, ETAs to the meter fixes and all active runways for all aircraft are first calculated. This step is highlighted in the box labeled “Calculate ETAs to meter fix and runways” in Figure 2. After calculating the ETAs, the flights are subsequently scheduled subject to the airport, meter fix, and runway constraints using the time-based TMA scheduling algorithm, which is a derivative of a first-come-first-served algorithm. Outcomes of this scheduling are scheduled times of arrival (STAs) to the meter fixes and active runways for all flights. These steps are captured in the box labeled, “Assign STAs to meter fix and runways” in Figure 2. The controls assigned by TMA at time t are labeled $u^{TMA}(t)$ in Figure 2 and consist of a set of airborne delays for the arriving flights. For simplicity these are implemented as airborne holding in the “Primary Simulation” system.

Fuel Burn and Emissions Modeling

The fuel burn and emissions model illustrated in Figure 2 uses the fuel consumption model in EUROCONTROL's Base of Aircraft Data Revision 3.7 (BADA) [EUROCONTROL, 2009]. The “Primary Simulation” (see Figure 2) provides aircraft information including aircraft type, mass, altitude and speed to compute the fuel burn (FB). There are five stages, climb, cruise, descent-idle, descent-approach, and descent-landing that are determined by the aircraft altitude, speed, and proximity to the arrival and departure airports. All but cruise and descent-idle stages use the following equation to calculate fuel burn

$$FB = SFC \cdot T \cdot \Delta t, \quad (1)$$

where FB is the fuel burn, SFC is the thrust specific fuel consumption, T is the trust, and Δt is the elapsed time. For cruise, the fuel burn is

$$FB = SFC \cdot T \cdot C_{fcr} \cdot \Delta t, \quad (2)$$

where C_{fcr} is the cruise fuel flow factor. For descent-idle, the fuel burn is

$$FB = C_{f3} \left(1 - \frac{h}{C_{f4}}\right), \quad (3)$$

where C_{f3} and C_{f4} are descent fuel flow coefficients, and h is the altitude.

After calculating FB, the emissions are subsequently calculated using the methodology developed for the FAA's System for assessing Aviation's Global Emissions (SAGE) [FAA, 2005]. Six emissions are computed including CO_2 , H_2O , SO_x , CO , HC and NO_x . Emissions of CO_2 , H_2O and SO_x (modeled as SO_2) are modeled based on fuel consumption [Hadaller and Momenthys, 1989]. The emissions are computed by

$$\begin{aligned} E_{CO_2} &= 3155 \cdot FB, \\ E_{H_2O} &= 1237 \cdot FB, \\ E_{SO_x} &= 0.8 \cdot FB, \end{aligned} \quad (4)$$

where E_{CO_2} , E_{H_2O} and E_{SO_x} are emissions of CO_2 , H_2O and SO_x in grams, and FB is fuel burn in kilograms.

Emissions of CO , HC and NO_x are modeled through the use of the Boeing Fuel Flow Method 2 (BFFM2) [Baughcum et al., 1996]. The emissions are determined by aircraft engine type, altitude, speed, and fuel burn and the coefficients in the International Civil Aviation

Organization (ICAO) emission data bank. In the models, fuel burn is corrected to sea-level reference temperature and pressure:

$$\begin{aligned} FB_C &= (FB / \delta_{amb}) [\theta_{amb}^{3.8} \exp(0.2M^2)], \\ \delta_{amb} &= P_{amb}/14.696, \\ \theta_{amb} &= (T_{amb} + 273.15)/273.15, \end{aligned} \quad (5)$$

where FB_C is the corrected fuel flow, P_{amb} is the at-altitude ambient pressure, T_{amb} is the at-altitude ambient temperature, and M is the Mach number. FB_C is used in ICAO emission data bank to determine the reference emission index $REIHC$, $REICO$ and $REINOx$ for HC, CO and NO_x . The emission indices are computed by

$$\begin{aligned} EICO &= REICO(\theta_{amb}^{3.3} / \delta_{amb}^{1.02}), \\ EIHC &= REIHC(\theta_{amb}^{3.3} / \delta_{amb}^{1.02}), \\ ECNOx &= REINOx[\exp(H)](\delta_{amb}^{1.02} / \theta_{amb}^{3.3})^{0.5}, \\ H &= -19.0(\omega - 0.0063), \end{aligned} \quad (6)$$

where $EICO$, $EIHC$ and $ECNOx$ are emission indices of CO, HC and NO_x , H is the humidity correction factor, and ω is the specific humidity.

The emissions are computed by

$$\begin{aligned} E_{CO} &= EICO \cdot FB, \\ E_{HC} &= EIHC \cdot FB, \\ E_{NOx} &= ECNOx \cdot FB, \end{aligned} \quad (7)$$

where, E_{CO} , E_{HC} and E_{NOx} are emission in gram.

EXPERIMENTAL SETUP

This section describes the TFP scenario, system inputs, and the TMA settings used for testing the integrated TFM approach proposed in the Modeling and Methodology section.

TFP Scenario

Traffic flow managers at the FAA's Air Traffic Control System Command Center developed the proposed TFP scenario used in this study. The intent of the TFP was to control arrivals destined for ATL prior to the flight entering the TMA freeze horizon when the arrival demand was forecasted to significantly exceed the arrival capacity during periods of taxiway construction. Taxiway construction at ATL began in September of 2010 and was expected to last throughout the fall of 2010. Without the use of a TFP under these circumstances, the

TMA, which is in operational use at ATL, could begin assigning significant airborne delays to flights in the en route environment and pre-departure delays to flights departing from within Atlanta Center. This can lead to significant inefficiencies and complexities in Atlanta Center's airspace, as controllers attempt to meet the schedules produced by TMA.

The FCA associated with the proposed TFP is illustrated in Figure 3 by the gray circle. This FCA consists of a 390 nmi circle centered around ATL. This radius was selected so that departures from airports, such as Orlando International Airport (MCO) and Indianapolis International Airport (IND), would be exempt (i.e., these flights would not be assigned any delays by the TFP) from the TFP. The radius of this circle is a parameter that is settable by the traffic management specialist, and this does not necessarily represent the "optimal" FCA radius for this study. Referring to Figure 3, all flights within the gray circle were exempt from the TFP, while flights outside the circle were included in the TFP and assigned CTAs (at the boundary of the FCA) and CTDs by FSM to accomplish a user-specified flow rate across the FCA boundary. Additionally, all flights originating from Canada were also exempt from the TFP. For modeling purposes, the TFP was assumed to begin at 11:00 am Eastern Daylight Time (EDT) and extend through 8:59 pm EDT, and the baseline flow rate across the TFP, as prescribed by traffic flow managers within the FAA, was assumed to be 54 aircraft per hour. As discussed in the Results section, this flow rate was subsequently

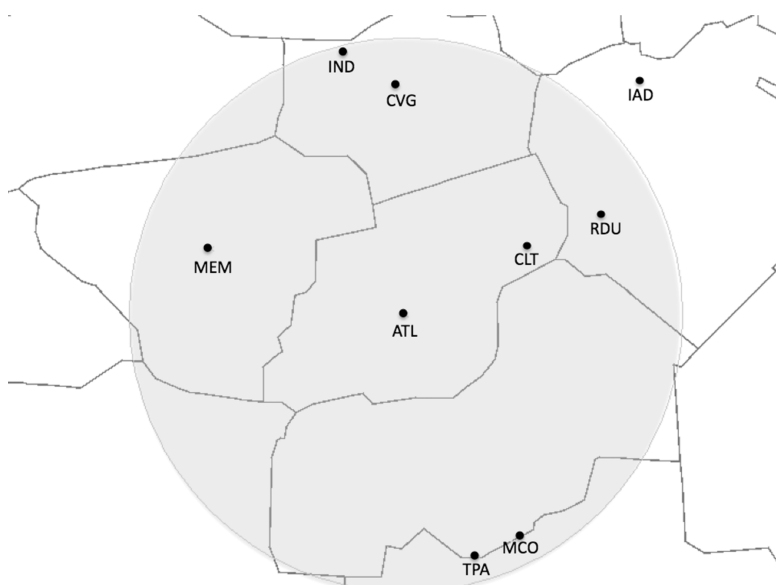


Figure 3. Proposed ATL Traffic Management Advisor Flow Program.

increased to 80 aircraft per hour to determine the most appropriate flow rate to use for a given ATL airport configuration.

System Inputs

The TFMS ADL file from June 29, 2010 was used in part to develop the nine hour and 59 minute scenario considered in this study. This file consisted of 571 ATL arrivals, 95 of which would have been exempt had the TFP been operationally implemented. As an aside, the set of flights exempt from the TFP is selectable by the traffic management specialist that is developing the TFP within FSM. For this particular TFP, the list of exempt flights included all flights departing from international airports and flights that were already airborne at the start of the TFP. It is worth noting that this list of flights only included arrivals that departed outside of the FCA (gray circle) depicted in Figure 3. The schedule for flights departing from within the FCA depicted in Figure 3 was developed using historical ASDI data archives from the June 29 and 30, 2010 ASDI data set. During the nine hour and 59 minute period starting on June 29th, a total of 418 flights departed for ATL from within this FCA. This data set was selected to coincide with the date of the ADL file that was used in planning the TFP that was previously described.

The unscheduled hourly ATL arrival demand between 11:00 am EDT and 8:59pm EDT is shown in Figure 4. The unfilled bars in Figure 4a correspond to the demand associated with the flights impacted by the TFP. It is worth noting that the number of TFP impacted flights is nearly zero in the first time bin (i.e., 11:00 am to 11:59 am), since it takes a flight roughly one hour to travel from the circumference of the FCA illustrated in Figure 3 to ATL. The hashed bars in Figure 4a correspond to the unscheduled demand associated with the flights exempt from the TFP. The total unscheduled demand is shown in Figure 4b. For reference, the nominal hourly airport arrival capacity of ATL when the airport is operating under the west-flow visual meteorological condition (VMC) configuration with three active runways is depicted by the dashed line in Figure 4b.

TMA Configuration

The TMA was operated in a west-flow VMC configuration with three active runways. The default airport arrival rate (AAR) under this configuration is 126 aircraft per hour. For reference, the five runways at ATL are labeled in Figure 5. For our experiments, 26R, 27L and 28 were used for arrivals and 26L and 27R were used for departures under the west-flow airport configurations. No east-flow configurations were considered, but when the airport is in this configuration, runways 8L, 8R, 9L, 9R and 10 are used. When

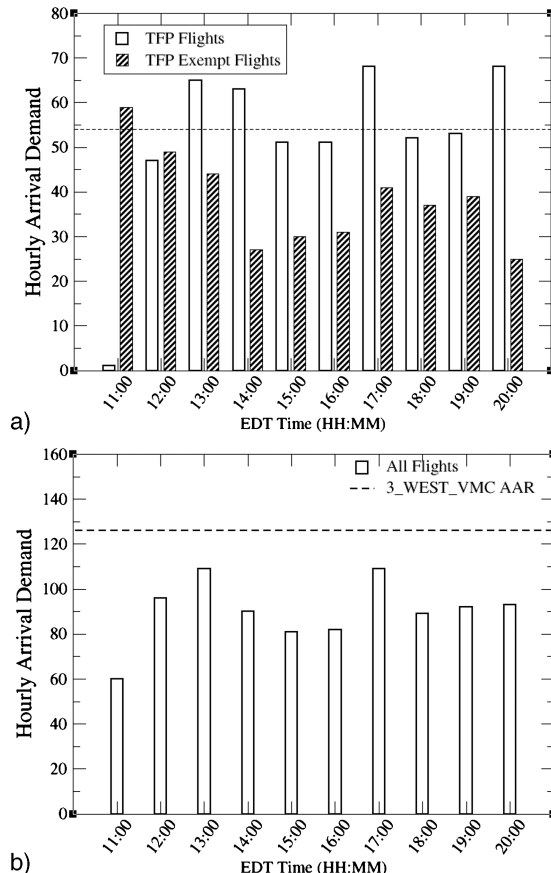


Figure 4. (a) Hourly unscheduled arrival demand for the TFP flights (white bars) and the flights exempt from the TFP (dashed bars) ATL arrival demand and (b) total unscheduled arrival demand between 11:00 and 20:59 EDT.

configuring the TMA, the acceptance rate at the airport, including all runways and gates, was set to be “unrestricted”, which is consistent with the way in which TMA is typically configured at ATL. “Unrestricted” in this case implies that only the minimum wake vortex separation requirements at the runways (see Table 1) were being enforced. Additionally, a five nautical miles (nmi) inter-aircraft spacing constraint was imposed at all meter fixes.

The default wake vortex separation matrix used for the active runways (i.e., 26L, 27R and 28) is shown in Table 1. The data in this table shows the minimum separation in nautical miles between aircraft as they land in order for the trailing aircraft to avoid the wake vortex of the leading aircraft. The leading aircraft type is specified in the first column of the table, while the trailing aircraft type appears in the subsequent columns. For example, the minimum spacing at the runway when a small turboprop follows a heavy jet is six nautical miles. The required wake vortex separation varies

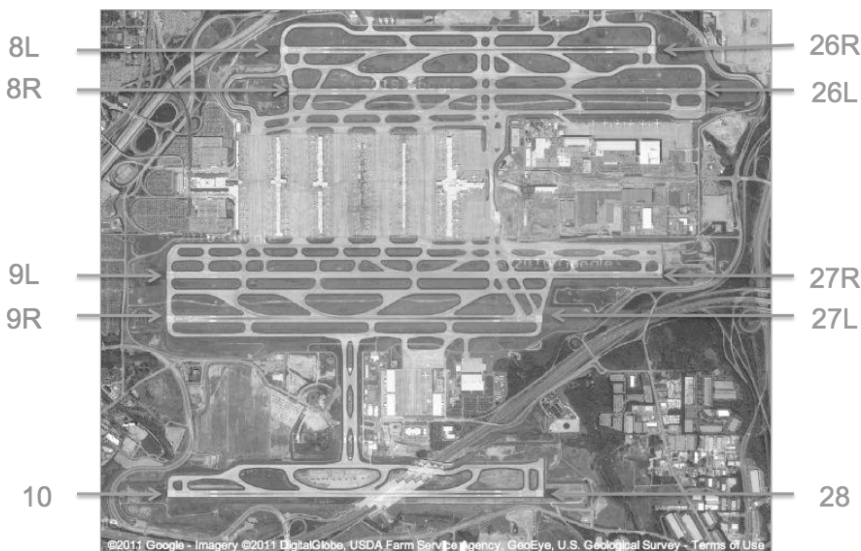


Figure 5. Airport Diagram for Hartsfield-Jackson Atlanta International Airport.

depending on the engine type and weight class of the two aircraft that are being separated.

RESULTS

This section contains the results of six, 10-hr, fast-time simulation experiments that were designed to examine the “best” flow rate associated with a TFP and to explore the environmental impact of TFPs on ATL arrival operations. For each of these experiments, the TMA was configured in the three runways, west-flow configuration that was previously described. The hourly flow rate associated with the TFP was allowed to take one of the following values: 54, 56, 60, 64, 72 and 80. The mean delays and total delay costs are presented in the Delay Variations with TFP Flow Rate subsection. The total fuel burn and emissions statistics for all flights arriving at ATL during the TFP are

Table 1. Default TMA Wake Vortex Separation Matrix (in nmi) with the First Column Indicating the Leading Aircraft Type and Subsequent Columns Indicating the Trailing Aircraft Type

	Heavy Jet	Large Jet	Large Turboprop	Small Turboprop	Small Piston	Boeing 757
Heavy Jet	4.0	5.0	5.0	6.0	6.0	5.0
Large Jet	2.5	2.5	2.5	4.0	4.0	2.5
Large Turboprop	2.5	2.5	2.5	4.0	4.0	2.5
Small Turboprop	2.5	2.5	2.5	2.5	2.5	2.5
Small Piston	2.5	2.5	2.5	2.5	2.5	2.5
Boeing 757	4.0	4.0	4.0	5.0	5.0	4.0

presented in the Fuel and Emission Variations with TFP Flow Rate subsection. Finally, the fuel burn and emission statistics associated with the TFM delays are presented in the TFM Related Fuel Burn and Emissions subsection.

Delay Variations with TFP Flow Rate

To determine the “best” TFP flow rate to use for a given arrival demand scenario, six fast-time simulations were completed in which the TFP flow rate was assigned one of the following values: 54, 56, 60, 64, 72 and 80 aircraft per hour. The 54 aircraft per hour scenario represents a situation in which the unscheduled, hourly arrival demand for flights included in the TFP exceeds this capacity limit for four of the ten hours that were considered, as illustrated by the white bars in Figure 4a. In contrast, the 80 aircraft per hour flow rate represents a situation in which the flights included in the TFP are essentially uncontrolled, so the only delays assigned to these flights are from the TMA.

Two alternative approaches were examined to determine the “best” TFP flow rate given the ATL arrival demand profile depicted in Figure 4. In the first approach, the total mean delays (e.g., includes both airborne and pre-departure delays) associated with the flights included and exempt from the TFP were examined. This approach was selected to attempt to balance the mean delays experienced by flights included and exempt from the TFP. To a certain degree, this approach attempts to ensure equity in the design of the TFP. In the second approach, a delay cost was calculated where presumably the “best” TFP flow rate would minimize the delay cost. In contrast to the first approach, this approach is focused on designing a TFP that preserves efficiency in the NAS. Here the delay cost in minutes is given by the following expression:

$$\text{DelayCost} = \text{GroundDelay} + w \times \text{Airborne Delay}$$

where $w \in \{1,2,3\}$. As is the usual convention, w is used to capture the additional costs (e.g., fuel costs) associated with operating an aircraft in the air, as opposed to being parked at the gate where the “GroundDelay” is incurred. Here “GroundDelay” is the delay assigned to flights by the TFP and the delay assigned to flights departing from within the TMA free horizon, which typically extends about 200 nmi from the airport. “AirborneDelay” is the delay assigned to flights by the TMA when the flight departs outside the TMA freeze horizon, which constitutes the vast majority of the flights.

Results for determining the “best” TFP flow rate by examining the mean flight delays are presented in Figure 6a. Here the mean flight delays are plotted as a function of the TFP flow rate for the TFP

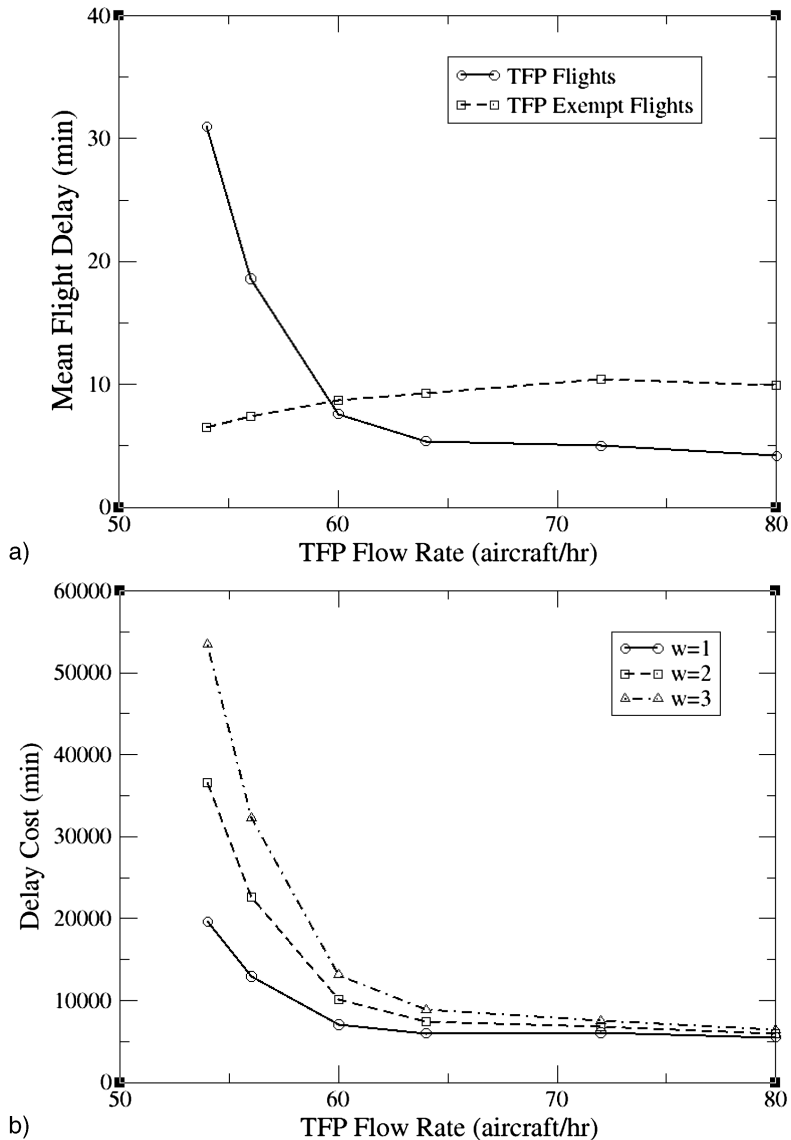


Figure 6. (a) Mean flight delay in minutes versus the TFP flow rate in aircraft per hour for the flights include (solid line) and exempt (dashed line) from the TFP and (b) delay cost in minutes versus the TFP flow rate with an airborne delay weighting factor of one (solid curve), two (dashed curve) and three (dot-dashed curve).

impacted flights (solid line) and the flights exempt from the TFP (dashed line). The mean delays for the flights exempt from the TFP, which are due entirely to the TMA, are shown to vary between 6.5 min and 10.4 min and they are only weakly correlated to the TFP flow rate. In contrast, the mean delays for the TFP impacted flights are strongly correlated with the TFP flow rates, and these delays are shown to decrease rapidly from 31.0 min per flight to 4.2 min per flight as the TFP flow rate is increased. Based on visual

inspection of Figure 6a, the “best” TFP flow rate is 60 aircraft per hour. Here the term “best” is used to indicate a TFP flow rate, which results in nearly equal mean flight delays for the flights impacted by the TFP and exempt from the TFP.

The results for determining the “best” TFP flow rate by examining the delay cost are presented in Figure 6b. As clearly indicated by this figure, if the intent is to minimize the delay cost, the best solution is to not implement a TFP, or to implement a TFP with a high flow rate. Clearly, these results are strongly influenced by a number of factors, such as the arrival demand and the airport configuration, and these results are not expected to hold in general.

Fuel and Emission Variations with TFP Flow Rate

To better understand the geographical distribution of the fuel burn and emissions associated with the 884 flights that were destined for ATL between 11:00 am EDT and 8:59 pm EDT, a uniform grid was created in FACET, which encompassed the entire United States, Canada, and Mexico. Individual grid cells measured 25 nmi x 25 nmi and extended from 24,000 ft to 99,999 ft. During the six, 10-hr fast time simulations that were previously mentioned, the following cumulative statistics were recorded in each grid cell: FB, CO₂ emissions, CO emissions, NO_x emissions, SO_x emissions and HC emissions. The results associated with the TFP with a flow rate of 54 aircraft per hour are shown in Figures 7.

The cumulative fuel burn (Figure 7a), CO₂ emissions (Figure 7b), CO emissions (Figure 7c), NO_x emissions (Figure 7d), SO_x emissions (Figure 7e) and HC emissions (Figure 7f) are presented in Figure 7. When comparing these six images, it is worth noting that the scales on the individual images vary dramatically. For example, the maximum CO₂ emissions observed in any one 25 nmi by 25 nmi cell exceeded 3,600 kg (see the black cells in Figure 7b), while the maximum cumulative SO_x emissions in one of these cells only exceeded 600 g (see the black cells in Figure 7e). The major ATL arrival flows converging over the four primary arrival fixes are clearly illustrated in this figure by the black cells. Additionally, traffic flows from eastern Canada, Mexico, and the west coast are distinguishable by the gray cells. As expected, the highest concentration of arrivals occurs in and around Atlanta Center.

For the simulations, the TFP only assigned pre-departure delays to the flights destined for ATL, so the TFM controls associated with the TFP would only affect the temporal distribution of the fuel burn and emissions results and not the cumulative results that are presented in Figure 7. The TMA, on the other hand, assigned pre-departure delays to flights departing from within the TMA freeze horizon, which typically extends about 200 nmi from the arrival airport, and

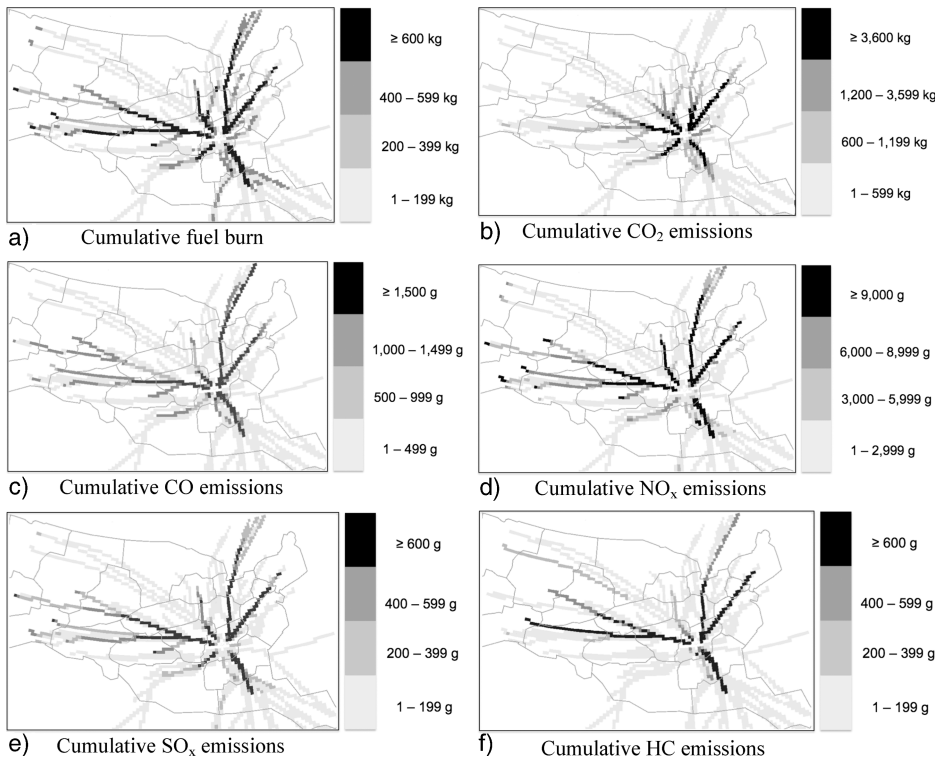


Figure 7. Cumulative fuel burn and emissions for ATL arrivals between 11:00 am EDT and 8:59 pm EDT.

airborne delays to all other flights. As mentioned in the Modeling Methodology section, the airborne delays are implemented as airborne holding at the ATL arrival meter fixes, so small variations in the fuel burn and emissions statistics near ATL are expected as the mix of ATL arrivals changes. This will be explored in more detail in the following subsection.

TFM Related Fuel Burn and Emissions

The influence of the TMA on the fuel burn and emissions for the six, 10-hr fast time simulations are presented in Figure 8. In each of these images, only the fuel burn or emissions associated with the TMA scheduling delays are being displayed as a function of the TFP flow rate. As is clearly illustrated in this figure, there is a strong correlation between the fuel burn and emissions and the TFP flow rate. This occurs because as the TFP flow rate increases, fewer flights are assigned pre-departure delays and more flights arrive in ATL Center at the same time, which require merging and spacing by the TMA. This in turn requires the TMA to assign more delays to the ATL arrivals to meet the arrival spacing constraints. This point is illustrated by the histogram of TMA delays that is shown in

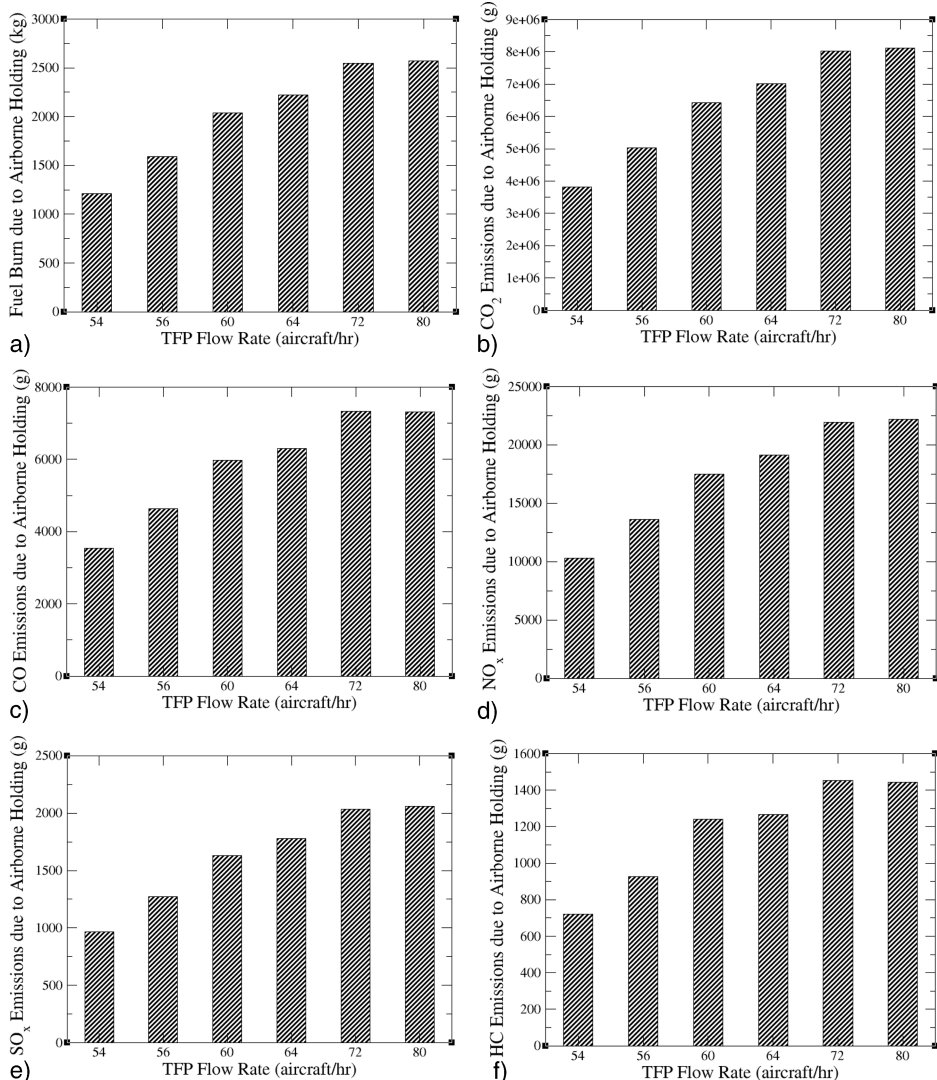


Figure 8. Fuel burn and emissions associated with the TMA delays for ATL arrivals between 11:00 am EDT and 8:59 pm EDT as a function of the TFP flow rate.

Figure 9a. Under all scenarios, the vast majority of flights receive less than five minutes of delay from the TMA; however, there is a noticeable increase in flights receiving more than 5 minutes of delay when the TFP flow rate is increased from 54 aircraft per hour to 64 aircraft per hour and 80 aircraft per hour. The average TMA delay under the three scenarios illustrated in this figure is: 3.01 minutes per flight when the TFP flow rate is 54 aircraft per hour, 5.15 min per flight when the flow rate is 64 aircraft per hour and 5.71 minutes per flight when the flow rate is 80 aircraft per hour. For completeness and to better illustrate the influence of the varying TFP flow rate on the pre-departure delays, the TFP delays

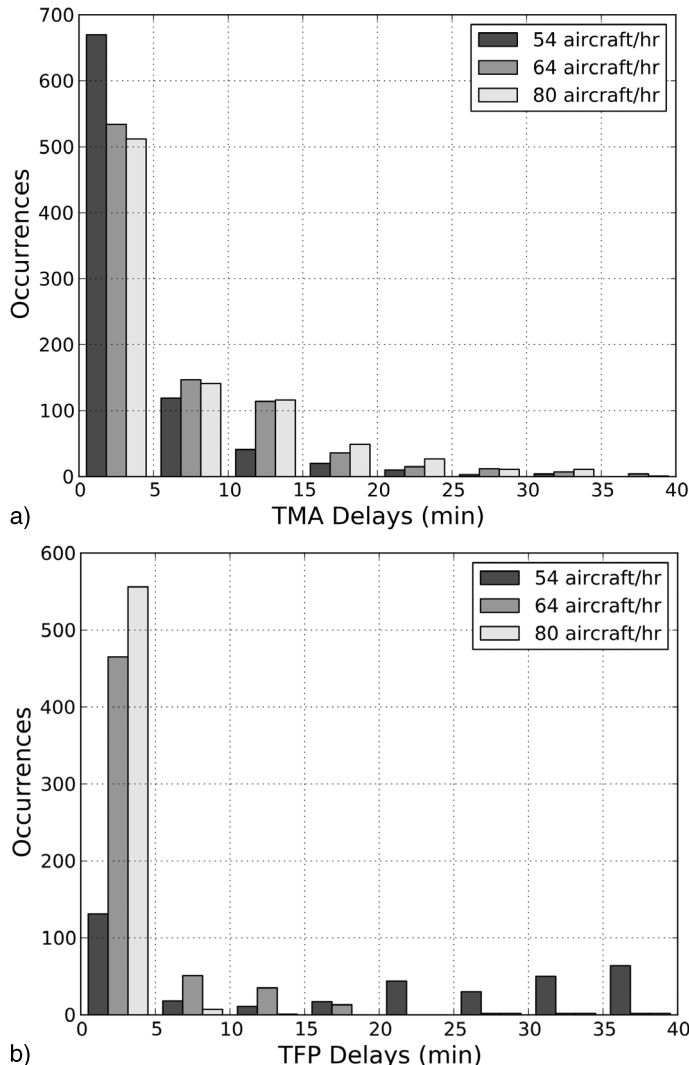


Figure 9. Histogram of (a) the TMA delays and (b) the TFP delays when the TFP flow rate is 54 aircraft per hour (dark gray bars), 64 aircraft (gray bars) and 80 aircraft/hr (light gray bars).

for the three aforementioned flow rates are illustrated in Figure 9b. This figure clearly illustrates that as the TFP flow rate increases; there is a corresponding decrease in the pre-departure, TFP delays. The average TFP delays under the three scenarios illustrated in Figure 9b follows: 29.95 minutes per flights when the TFP flow rate is 54 aircraft per hour, 2.54 minutes per flight when the flow rate is 64 aircraft per hour, and 0.81 minutes per flight when the flow rate is 80 aircraft per hour.

The net impact of these increasing delays, as illustrated by the results in Figure 8, is a 112% increase in fuel burn associated with the airborne delays assigned by the TMA when the TFP flow rate

increases from 54 aircraft per hour to 80 aircraft per hour (see Figure 8a); a 112% increase in the CO₂ emissions (see Figure 8b); a 107% increase in the CO emissions (see Figure 8c); a 116% increase in the NO_x emissions (see Figure 8d); a 112% increase in SO_x emissions (see Figure 8e) and a 100% increase in HC emissions (see Figure 8f). It is worth noting that these increases in fuel burn and emissions represent a small percent of the total fuel burn and emissions associated with the entire flight's trajectory, and only a percent of all arrivals were subject to these increases. So, as the environmental impact of aviation on the environment becomes a more pressing matter, the design of TFM control strategies will require not only a consideration of the delays associated with those strategies (see Figure 5), but also the emissions resulting from those strategies.

CONCLUSIONS

In 2010, the FAA investigated the use of a capability called a TFP, to reduce the demand of flights destined for a capacity-limited airport by using a new method to assign pre-departure delays to these flights. Here the flights controlled by the TFP depart from outside of the TMA scheduling horizon, which typically extends about 200 nmi from the airport. The final sequencing and scheduling of the arrivals within approximately 200 nmi of the airport is accomplished completely independently by the TMA. This study is designed to explore through fast-time simulations the delays and environmental impacts associated with first controlling flights with a TFP and subsequently by the TMA.

In an effort to determine the "best" flow rate to use for a given airport configuration and arrival demand scenario, the TFP was modeled with flow rates of 54, 56, 60, 64, 72 and 80 aircraft per hour. When the "best" flow rate was selected by balancing the mean delay incurred by flights included and exempt from the TFP, then the "best" TFP flow rate was 60 aircraft per hour. If however a TFP was to be designed that minimized the weighted sum of all ground delays and airborne delays then the best flow rate was 80 aircraft per hour.

Lastly, the magnitude and geographical distribution of the fuel burn and emissions associated with the 884 flights that were destined for ATL between 11:00 am EDT and 8:59pm EDT was analyzed. A strong correlation between the TFP flow rate and the fuel burn and emissions associated with the TMA delays was observed. When the TFP flow rate was increased from 54 aircraft per hour to 80 aircraft per hour, the fuel burn and emissions associated with the TMA delays was found to increase by over 100%. In general, these increases in fuel

burn and emissions represent a small percent of the total fuel burn and emissions associated with the flight's entire trajectory, and only a percent of all arrivals were subject to these increases. TFM control strategies have traditionally focused on improving efficiency (i.e., reducing delays) of air traffic operations. However, as aviation's impact on the environment becomes a more pressing matter, the design of TFM control strategies will require considering delays as well as emissions resulting from those strategies.

ACKNOWLEDGMENTS

The authors would like to thank Mrs. Kapri Kupper and Mr. Dwight MacConnell from the FAA for motivating this problem. Additionally, the authors are indebted to Mr. Liang Chen, Mr. Lee Helmle, Mr. Jim Murphy, and Mrs. Cynthia Freedman for sharing their expertise with NASA's Center TRACON Automation System and the Traffic Management Advisor.

ACRONYMS

AAR	Airport Arrival Rate
ADL	Aggregate Demand List
API	Application Programming Interface
ASDI	Aircraft Situation Display to Industry
ATL	Hartsfield-Jackson Atlanta International Airport
BADA	Base of Aircraft Data
BFFM2	Boeing Fuel Flow Method 2
CTA	Controlled Time of Arrival
CTD	Controlled Time of Departure
EDT	Eastern Daylight Time
ETA	Estimated Time of Arrival
EWR	Newark Liberty International Airport
FACET	Future ATM Concepts Evaluation Tool
FB	Fuel Burn
FCA	Flow Constrained Area
FSM	Flight Schedule Monitor
GDP	Ground Delay Program
ICAO	International Civil Aviation Organization
IND	Indianapolis International Airport
MCO	Orlando International Airport
NAS	National Airspace System
RBS	Ration by Schedule
SAGE	System for assessing Aviation's Global Emissions
STA	Scheduled Time of Arrival
TFMS	Traffic Flow Management System
TFP	TMA Flow Program
TMA	Traffic Management Advisor
VMC	Visual Meteorological Condition

REFERENCES

- Baughcuma, S., Tritz, T., Henderson, S. and Pickett, D. (1996), "Scheduled Civil Aircraft Emission Inventories for 1992: Database Development and Analysis," Project Report NASA CR 4700, April.
- Bilimoria, K. D., Sridhar, B., Chatterji, G., Sheth, K. S. and Grabbe, S. R. (2001), "Future ATM Concepts Evaluation Tool," *Air Traffic Control Quarterly*, Vol. 9, No. 1, March.
- Duquette, M. and Lacher, E. (2010), "Operational Analysis of Metering," Report No. MP100189, The MITRE Corporation, McLean, VA, June.
- "Enhanced Traffic Management System (ETMS)" (2005), Report No. VNTSC-DTS56-TMS-002, Volpe National Transportation Center, U.S. Department of Transportation, Cambridge, MA, Oct.
- EUROCONTROL Validation Infrastructure Centre of Expertise (2009), France, *User manual for the base of aircraft data (BADA)*, 3rd ed., March.
- Federal Aviation Administration (FAA) (2005), Washington, DC, *SAGE System for assessing Aviation's Global Emissions Technical Manual*, 1st ed., September.
- Grabbe, S., Sridhar, B. and Mukherjee, A. (2009), "Sequential Traffic Flow Optimization with Tactical Flight Control Heuristics," *AIAA Journal of Guidance, Control and Dynamics*, Vol. 32, No. 3, pgs. 810-820, May-June.
- Grabbe, S., Sridhar, B., Mukherjee, A. and Morando, A. (2010), "Interaction Between Strategic and Local Traffic Flow Controls," *AIAA Guidance, Navigation and Control Conference*, Toronto, Canada, AIAA Paper 2010-8073, Aug. 2-5.
- Grabbe, S., Sridhar, B., Mukherjee, A. and Morando, A. (2011), "Traffic Management Advisor Flow Programs: an Atlanta Case Study," *AIAA Guidance, Navigation and Control Conference*, Portland, OR, Aug. 8-11.
- Hadaller O. J. and Momently, A. M. (1989), "The Characteristics of Future Fuels," Project Report D6-54940, Boeing publication.
- Sridhar, B., Chen, N. Y., Ng, H. K. and Morando, A. (2011), "Modeling and Simulation of the Impact of Air Traffic Operations on the Environment," *AIAA Modeling and Simulation Technologies Conference*, Portland, OR, Aug. 8-11.
- Swenson, H. N., T. Hoang, Engelland, S., Vincent, D., Sanders, T., Sanford, B. and Heere, K. (1997), "Design and Operational Evaluation of the Traffic Management Advisor at the Fort Worth Air Route Traffic Control Center," *1st Eurocontrol/FAA ATM R&D Seminar*, Saclay, France, June 17-19.

BIOGRAPHIES

Shon R. Grabbe received his Ph.D. in atomic physics from Kansas State University in 1997. He currently serves as the Technical Lead for NASA's Traffic Flow Management research activities. Since graduation, Dr. Grabbe has been responsible for conducting and leading research activities in the area of air traffic management. He has over 50 conference and journal publications in the fields of atomic physics and air traffic management. Shon is an Associate Fellow of the American Institute of Aeronautics and Astronautics. Additionally, he is the co-inventor of a U.S. Patent entitled, "Air Traffic Management Evaluation Tool." In 2006, Shon was a recipient of NASA's Software of the Year Award, and in 2009 he received the American Institute of Aeronautics and Astronautics Software Engineering Award. His current research interests are in the application of modeling and optimization techniques to aerospace systems.

Banavar Sridhar received the B.E. degree in electrical engineering from the Indian Institute of Science and the M.S. and Ph.D. in electrical engineering from

the University of Connecticut. He worked at Systems Control, Inc., Palo Alto, CA and Lockheed Palo Alto Research Center before joining NASA Ames Research Center in 1986. He is NASA Senior Scientist for Air Transportation Systems. His research interests are in the application of modeling and optimization techniques to aerospace systems. Dr. Sridhar received the 2004 IEEE Control System Technology Award for his contributions to the development of modeling and simulation techniques for multi-vehicle traffic networks. He led the development of traffic flow management software, Future ATM Concepts Evaluation Tool (FACET), which received the NASA Invention of the Year Award in 2010 and the AIAA Engineering Software Award in 2009. He is a Fellow of the IEEE and the AIAA.

Avijit Mukherjee is an Associate Research Scientist at the University Affiliated Research Center, NASA Ames Research Center, Moffett Field, CA. He received his Ph.D. in Civil and Environmental Engineering from University of California, Berkeley. He was a Research Associate at the Institute for Systems Research, University of Maryland at College Park, from 2004 to 2006. Dr. Mukherjee's research focuses on air transportation, simulation, optimization, and statistical modeling of transportation systems. He has published more than 30 journal and conference articles.

Alexander Morando is a Senior Software Engineer at the University Affiliated Research Center, NASA Ames Research Center, Moffett Field, CA. He received his BSME/MSME degrees from the University of California, Berkeley. He was previously an ECS Simulation Engineer at Honeywell Aerospace, Torrance, CA. His interests include control systems theory, dynamic simulation, and object-oriented software design.